



**HAL**  
open science

## Changes in hydrogenase genetic diversity and proteomic patterns in mixed culture dark fermentation of mono-, di- and tri-saccharides

Marianne Quéméneur, Jérôme Hamelin, Saida Benomar, Marie-Thérèse Guidici-Orticoni, Eric Latrille, Jean-Philippe Steyer, Eric Trably

### ► To cite this version:

Marianne Quéméneur, Jérôme Hamelin, Saida Benomar, Marie-Thérèse Guidici-Orticoni, Eric Latrille, et al.. Changes in hydrogenase genetic diversity and proteomic patterns in mixed culture dark fermentation of mono-, di- and tri-saccharides. *International Journal of Hydrogen Energy*, 2011, 36 (18), pp.11654-11665. 10.1016/j.ijhydene.2011.06.010 . hal-00677381

**HAL Id: hal-00677381**

**<https://hal.science/hal-00677381>**

Submitted on 8 Aug 2023

**HAL** is a multi-disciplinary open access archive for the deposit and dissemination of scientific research documents, whether they are published or not. The documents may come from teaching and research institutions in France or abroad, or from public or private research centers.

L'archive ouverte pluridisciplinaire **HAL**, est destinée au dépôt et à la diffusion de documents scientifiques de niveau recherche, publiés ou non, émanant des établissements d'enseignement et de recherche français ou étrangers, des laboratoires publics ou privés.

1 Changes in hydrogenase genetic diversity and proteomic patterns in mixed-culture dark  
2 fermentation of mono-, di- and tri-saccharides

3

4 Marianne Quéméneur<sup>1</sup>, Jérôme Hamelin<sup>1</sup>, Saida Benomar<sup>2</sup>, Marie-Thérèse Guidici-Ortoni<sup>2</sup>,  
5 Eric Latrille<sup>1</sup>, Jean-Philippe Steyer<sup>1</sup>, and Eric Trably<sup>1\*</sup>

6

7

8 Author addresses

9 <sup>1</sup> INRA, UR050, Laboratoire de Biotechnologie de l'Environnement, avenue des Etangs,  
10 Narbonne, F-11100, France

11 <sup>2</sup> Laboratoire de Bioénergétique et Ingénierie des Protéines, UPR 9036, IFR 88, CNRS 31  
12 chemin Joseph Aiguier 13402 Marseille cedex 20, France

13

14 \* Corresponding author:

15 Tel.: +33(0)468425151; Fax: +33(0)468425160; E-mail address: [trably@supagro.inra.fr](mailto:trably@supagro.inra.fr);

16 **Abstract**

17

18 Dark fermentation using mixed cultures is a promising biotechnology for producing hydrogen  
19 (H<sub>2</sub>) from renewable organic waste at a low cost. The impact of the characteristics of  
20 carbohydrates was evaluated on H<sub>2</sub> production and the associated changes in clostridial  
21 populations. A series of H<sub>2</sub>-producing batch experiments was performed from mono-, di- to  
22 tri-saccharides (i.e. fructose, glucose, sucrose, maltose, cellobiose, maltotriose). Both chain  
23 length and alpha- or beta-linkage of carbohydrates impacted H<sub>2</sub> production performance as  
24 well as the patterns of hydrogenases. The H<sub>2</sub> yield, ranging from 1.38 to 1.84 mol-H<sub>2</sub>/mol-  
25 hexose, decreased with the increasing chain length of the carbohydrates, showing a negative  
26 effect of the hydrolysis step on H<sub>2</sub> production efficiency. Changes in H<sub>2</sub> yield were associated  
27 with a specialization of clostridial species, which used different metabolic routes. The rise in  
28 H<sub>2</sub> production was associated with butyrate and acetate increases while H<sub>2</sub> consumption was  
29 related to caproate formation. Both clostridial [FeFe]- and [NiFe]-hydrogenases were  
30 identified in cellobiose cultures by a proteomic approach. This is the first study that combines  
31 genetic and proteomic analyses focused on H<sub>2</sub>-producing bacteria under various conditions  
32 and it opens very interesting perspectives to better understand and optimize H<sub>2</sub> production  
33 using mixed cultures.

34

35 **Keywords:** hydrogen, *Clostridium*, CE-SSCP, *hydA* functional genes, anaerobic digestion,  
36 substrate

## 37 **1. Introduction**

38

39 Hydrogen ( $H_2$ ) is one of the most promising, clean and renewable energy carriers. In recent  
40 years, considerable effort has been made to improve biological technologies for efficient,  
41 economic and renewable  $H_2$  production [1, 2]. For large-scale  $H_2$  production, dark  
42 fermentation processes using mixed cultures have some essential advantages over other  
43 bioprocesses: these include low energy requirements, high rates of production and  
44 considerable versatility of the organic substrates. Both purified sugar substrates and solid,  
45 waste-derived carbon sources, such as agricultural [3], food [4] or industrial waste [5], have  
46 been used to produce  $H_2$ . However, the main drawback of fermentative processes is the low  
47 yield of  $H_2$  per mole of organic substrate consumed. To date, several strategies, such as  
48 metabolic pathway control or fermentation process optimization, have been proposed in the  
49 literature for improving  $H_2$  production yields [1, 6, 7].

50 The  $H_2$  production yield *via* dark fermentation varies widely according to the type of carbon  
51 substrate, the operating conditions and the type of  $H_2$ -producing bacteria (HPB) involved [8,  
52 9]. Mixed cultures are potentially more suitable for degrading a wide range of complex and  
53 unsterile substrates. However,  $H_2$  is a metabolic intermediate in anaerobic mixed cultures and  
54 is rapidly reused by  $H_2$ -consuming microorganisms (HCM). Therefore, in mixed cultures, the  
55  $H_2$  yields are not only influenced by the metabolic switches in bacterial cells but also by the  
56 population equilibrium between HPB and HCM [10]. Improvement in  $H_2$  production yields  
57 using mixed cultures also relies heavily on microbial community dynamics which can respond  
58 to variations in operating conditions either by metabolic adaptation and/or by fluctuation in  
59 community composition. Moreover, HPB compete for selective carbohydrate uptake and  
60 metabolism to acquire a competitive advantage over other microorganisms [11, 12]. However,

61 only a few studies have reported changes in HPB population composition associated with  
62 changes in carbon sources [13, 14].

63 Previous studies of microbial communities have shown that HPB mixed cultures are usually  
64 dominated by clostridial species. This is due to heat treatment of the inoculum or the short  
65 hydraulic retention times often used to eliminate HCM (e.g. methanogens) [2, 15-18]. In fact,  
66 the clostridial species are recognized as effective H<sub>2</sub>-producers using a wide range of  
67 carbohydrate substrates. Alterations in the functioning of ecosystem (such as a decrease in the  
68 H<sub>2</sub> yield in dark fermentation) are often associated with changes in the metabolism and  
69 composition of microbial communities [15, 16, 19, 20]. By way of example, shifts in  
70 microbial community from H<sub>2</sub>-producing clostridial species to competitor HCM or non-H<sub>2</sub>-  
71 producing bacteria such as lactic acid bacteria have been observed concomitantly with process  
72 instability. Such fluctuations can include H<sub>2</sub> production failure or variations in metabolite  
73 concentrations in the anaerobic bioreactors [21]. Some clostridial species are able to switch  
74 from H<sub>2</sub>/acids to solvent production depending on the operating conditions [22, 23]. The  
75 metabolic flexibility of clostridial species leads to the production of a wide range of end  
76 products. Such variety may lower the H<sub>2</sub> yield from the theoretical maximum of 4 mol-  
77 H<sub>2</sub>/mol-hexose which is obtained when acetate is the sole end product from fermentation. The  
78 genus *Clostridium* is a large and phenotypically heterogeneous bacterial group containing  
79 carbohydrate-fermenters, protein-fermenters and homoacetogens, all of which have not been  
80 phylogenetically well defined [24, 25]. H<sub>2</sub>-producing and H<sub>2</sub>-consuming clostridial species  
81 are in fact closely related phylogenetically, although they follow opposite physiological  
82 pathways [25, 26]. Consequently, changes in clostridial community make-up underlying  
83 changes in H<sub>2</sub> production performance can be difficult to observe using 16S rRNA gene-  
84 based methods [10, 16, 27].

85 H<sub>2</sub> production is catalyzed by the enzymatic activity of hydrogenases (H<sub>2</sub>ases) which are  
86 classified in two major phylogenetically distinct classes according to their bimetallic center of  
87 the catalytic site: [NiFe]-H<sub>2</sub>ases and [FeFe]-H<sub>2</sub>ases [28]. While [NiFe]-H<sub>2</sub>ases tend to be  
88 involved in H<sub>2</sub> consumption, [FeFe]-H<sub>2</sub>ases are usually involved in H<sub>2</sub> production [28].  
89 Indeed, in mixed cultures, the *hydA* genes, encoding the catalytic subunit of [FeFe]-H<sub>2</sub>ases,  
90 have already been used as pertinent molecular markers of HPB in mixed cultures [16, 20, 29],  
91 in relation to changes in H<sub>2</sub> production performances [16, 29, 30]. Moreover, in relation to  
92 monitoring changes in H<sub>2</sub> production performances, the *hydA* population shifts have been  
93 reported as more sensitive than shifts in overall bacterial population [10, 20].  
94 The aim of this study was to assess the impact of characteristics of carbohydrates on the  
95 bacterial population and on the metabolic changes associated with fermentative H<sub>2</sub>  
96 production. To this end, we evaluated the impact on H<sub>2</sub> production performances of  
97 carbohydrate chain length and alpha or beta linkages using mesophilic mixed cultures. The  
98 metabolic routes and the diversity of H<sub>2</sub>ases used to produce or consume H<sub>2</sub> have also been  
99 discussed in the light of genetic and proteomic approaches.

## 100 **2. Materials and methods**

101

### 102 **2.1. Hydrogen production in batch tests**

103

104 The H<sub>2</sub> production experiments were carried out in 500 mL glass bottles under batch  
105 conditions. The inoculum corresponded to an anaerobically-digested sludge pretreated by  
106 heat/shock treatment (90°C, 10 min). Two milliliters of the pretreated inoculum (final  
107 concentration of 225 mg-COD/L) were inoculated into the culture medium (final working  
108 volume of 200 mL) containing 40 mM of 2-(N-morpholino)ethanesulfonic acid (MES) buffer  
109 and 10 g/L of the following carbohydrates: glucose (C<sub>6</sub>H<sub>12</sub>O<sub>6</sub>, molar mass (M) = 180.2 g/mol,  
110 Sigma), fructose (C<sub>6</sub>H<sub>12</sub>O<sub>6</sub>, M = 180.2 g/mol, Sigma), sucrose (C<sub>12</sub>H<sub>22</sub>O<sub>11</sub>, M = 342.3 g/mol,  
111 Rectapur), maltose (C<sub>12</sub>H<sub>22</sub>O<sub>11</sub>, M = 360.2 g/mol, Sigma), cellobiose (C<sub>12</sub>H<sub>22</sub>O<sub>11</sub>, M = 342.3  
112 g/mol, Sigma) or maltotriose (C<sub>18</sub>H<sub>32</sub>O<sub>16</sub>, M = 504.4 g/mol, Sigma). The choice of the type of  
113 carbohydrate was based on the variety of potential substrates retrieved after hydrolysis of  
114 different renewable materials. Sucrose, a disaccharide consisting of one glucose monomer and  
115 one fructose monomer linked  $\alpha$ -1,2, occurs naturally in various plant sources such as  
116 sugarcane or sugar beets. Maltose and cellobiose, both disaccharides consisting of two  
117 glucose monomers, the first linked  $\alpha$ -1,4, the second linked  $\beta$ -1,4, are also both the products  
118 of the hydrolysis of polysaccharides: maltose comes from starch, cellobiose comes from  
119 cellulose. Maltotriose, a trisaccharide consisting of three glucose monomers linked  $\alpha$ -1,4, is  
120 representative of linear glucose oligomers containing more than two units. The initial pH was  
121 adjusted to 5.5 using NaOH (1M). All batch tests were performed in triplicate. After  
122 inoculation, each bottle was flushed with nitrogen for 5 minutes to maintain anaerobic  
123 conditions. The bottles were then capped with a rubber stopper and incubated at 37°C for 14  
124 days. Four milliliters of the mixed cultures were periodically collected and then centrifuged

125 (20,000 g, 10 min). The supernatants and the pellets were stored at -20°C, the supernatants for  
126 further chemical analysis and the pellets for DNA extraction.

127

## 128 **2.2. Chemical data analysis (biogas, metabolic byproducts)**

129

130 The volume of biogas was daily measured using an acidified water displacement method.

131 Biogas composition (CH<sub>4</sub>, CO<sub>2</sub>, H<sub>2</sub> and N<sub>2</sub>) was determined by gas chromatography (GC-  
132 14A, Shimadzu) as previously described by Aceves-Lara *et al.* [7].

133 Volatile fatty acids (VFA) composition in the liquid phase, *i.e.* acetic (C2), propionic (C3),  
134 butyric and iso-butyric (C4 and iC4), valeric and iso-valeric (C5 and iC5) and caproic (C6)  
135 acids were determined with a gas chromatograph (GC-3900, Varian) equipped with a flame  
136 ionization detector. The concentrations of carbohydrates and non-VFAs metabolic byproducts  
137 such as organic acids (lactate), ethanol or acetone were assessed by HPLC analysis and a  
138 refractometer (Waters R410). The compounds were separated using an Aminex HPX-87H,  
139 300 x 7.8 mm column (Biorad). The column temperature was maintained at 35°C and the  
140 flow rate at 0.4 mL/min. Substrate degradation efficiency was estimated by dividing the  
141 amount of carbohydrate consumed by the amount of initial carbohydrate.

142 To determine the H<sub>2</sub> production performances obtained for the different carbohydrates (Table  
143 1), the cumulative H<sub>2</sub> production (H) data for each carbohydrate was fitted to a modified  
144 Gompertz equation (1) as shown in Figure 1.

$$145 \quad H(t) = P \cdot \exp \left\{ -\exp \left[ \frac{R_m \cdot e}{P} (\lambda - t) + 1 \right] \right\} \quad (1)$$

146 where  $P$  is the H<sub>2</sub> production potential (mL/L),  $R_m$  is the maximum H<sub>2</sub> production rate  
147 (mL/L/day),  $\lambda$  is lag-phase time (day),  $t$  is the incubation time (day) and  $e$  is  $\exp(1)$ . The  
148 cumulative H<sub>2</sub> production was expressed in mL per L of culture taking into account the  
149 volume variations due to gas and liquid samplings. The values of  $P$ ,  $R_m$  and  $\lambda$  were estimated



150 using a non-linear regression algorithm developed in Matlab (version 6.5, Mathworks). The  
151 H<sub>2</sub> consumption rate (R<sub>c</sub>) was evaluated by the H<sub>2</sub> decrease measured in experiments between  
152 the P time and the end of the experiments. The H<sub>2</sub> production yield was calculated by dividing  
153 the maximum H<sub>2</sub> production potential (*P*) by the mol of hexose-equivalent consumed.

154

### 155 **2.3. DNA extraction and PCR amplification**

156

157 For each experiment, molecular analyses of the bacterial communities were carried out in  
158 triplicate at the start of the experiments (initial time), at the H<sub>2</sub> production potential stage (*P*)  
159 and at the end of the experiments (after 14-day incubation).

160 Genomic DNA was extracted and purified from cell pellets using the Wizard Genomic DNA  
161 Purification kit (Promega). The amount and purity of DNA in the extracts were measured by  
162 spectrophotometry (Infinite NanoQuant M200, Tecan).

163 The *hydA* genes were amplified using the non-degenerated primers [16] *hydAClosF* (5' –  
164 ACCGGTGGAGTTATGGAAGC – 3', *C. pasteurianum* position F1258) and 5'-fluorescein  
165 phosphoramidite-labeled *hydAClosR* (5' – CATCCACCTGGACATGCCAT – 3', *C.*  
166 *pasteurianum* position R1508). Each PCR mixture (50 µL) contained 1X *Pfu* Turbo DNA  
167 polymerase buffer, 200 µM of each dNTP, 0.5 µM of each primer, 0.5 U of *Pfu* Turbo DNA  
168 polymerase (Stratagene) and 1 ng of genomic DNA. Reactions were done in a Mastercycler  
169 thermal cycler (Eppendorf). The *hydA* genes were amplified as follows: 94 °C for 2 min,  
170 followed by 35 cycles performed at 94 °C for 30 s, 57 °C for 30 s, and 72 °C for 30 s, with a  
171 final extension at 72 °C for 10 min.

172 The 16S rRNA genes were amplified using the universal primers W49 (5'-  
173 ACGGTCCAGACTCCTACGGG-3', *Escherichia coli* position F331) [31] and 5'-fluorescein  
174 phosphoramidite-labeled W104 (5'-TTACCGCGGCTGCTGGCAC-3', *E. coli* position R533)

175 [31], as described above, except that 25 cycles and primer hybridization at 61 °C were applied  
176 and 130 ng of each primer were used. The *Clostridium* genus was specifically analyzed by  
177 nested PCR using a bacterial-domain forward primer W18 (5'-  
178 GAGTTTGATCMTGGCTCAG -3', *E. coli* position F9) [32] and a *Clostridium*-specific  
179 reverse primer W109 (5'- CCCTTTACACCCAGTAA -3', *E. coli* position R561) [33, 34].  
180 The size of PCR products (200 bp) was determined by 2% gel electrophoresis stained with  
181 ethidium bromide.

182

#### 183 **2.4. CE-SSCP electrophoresis and statistical analysis**

184

185 *Electrophoresis*- One microliter of appropriate dilution of PCR product was mixed with 18.8  
186 µL of formamide and 0.2 µL of internal standard GeneScan ROX (Applied Biosystems).  
187 Samples were heat-denatured at 95°C for 5 min and immediately cooled in ice. CE-SSCP  
188 electrophoresis was performed in an ABI Prism 3130 genetic analyser (Applied Biosystems)  
189 with 50 cm-long capillary tubes filled with a non-denaturing 5.6% conformation analysis  
190 polymer (Applied Biosystems). Samples were eluted at 12 kV and 32°C for 30 min (for 16S  
191 rRNA gene) or 45 min (for *hydA* gene).

192 *Data analysis*- The CE-SSCP profiles were aligned with the internal standard to take into  
193 account inter-sample electrophoretic variability. The CE-SSCP profiles were normalized  
194 using the StatFingerprints library [35] from R version 2.9.2 [36] in accordance with standard  
195 procedure [37]. The genetic distances between bacterial communities were assessed using  
196 Euclidean distances. The effect of the type of carbohydrate on the structure of bacterial  
197 communities was investigated with a multivariate analysis of similarity (ANOSIM) [38].  
198 ANOSIM gives a statistic, R, ranging from 0 (dissimilar groups) to 1 (similar groups). The  
199 statistical significance of R was tested by Monte Carlo randomization. The complexity of the

200 bacterial community was estimated using Simpson's diversity index from a CE-SSCP profile  
201 taking into account the number of species (number of peaks) as well as their relative  
202 abundance (area under each peak) [39].

203

## 204 **2.5. Assignment of the partial *hydA* sequences in mixed cultures**

205

206 The PCR products obtained from the H<sub>2</sub>-producing mixed cultures were purified using a PCR  
207 Purification Kit (Qiagen). The *hydA* clone libraries were constructed using the TA Cloning  
208 Kit (Invitrogen). The PCR-CE-SSCP profile of each PCR product, amplified using plasmid-  
209 targeted primers T7 and P13, was compared with the HPB culture profiles for peak  
210 assignment. The cloned inserts were sent for sequencing (MilleGen Company, Toulouse,  
211 France). The protein sequences, deduced from the nucleotide *hydA* sequences, were aligned  
212 with reference sequences retrieved from the Genbank database using the CLUSTALW  
213 program [40] then further refined manually using the BioEdit program [41]. Distances were  
214 estimated by the Kimura method [42] and the neighbor-joining method was used for inferring  
215 the tree topologies [43]. Tree topology confidence was determined by bootstrap analysis on  
216 1000 replicates [44]. All phylogenetic programs were implemented with SeaView software  
217 [45]. The *hydA* gene sequences were deposited in the Genbank database under the accession  
218 numbers JF714976 to JF714980.

219

## 220 **2.6. Protein electrophoresis and proteomic data analysis**

221

222 *Electrophoresis*- Cell material was collected at the end of the experiment (14 days). Soluble  
223 proteins released from dead bacterial cells were eliminated prior to protein extraction by  
224 rinsing cell pellets. Washed pellets were resuspended in 50mM Tris-HCl, 10 µg/ml Dnase,

225 5% glycerol and proteases inhibitors (pH 7.6) (bufferA), mutanolysin (200U/ml) (Roche) and  
226 incubated 1hour at 37°C under argon. After centrifugation (30 min 3700g, 4°C), cell material  
227 was resuspended in buffer A and broken in a French cell press. Debris and unbroken cells  
228 were removed by centrifugation (10000g, 15 min). Membrane and soluble proteins were  
229 separated by ultracentrifugation (45 min, 40000 rpm, rotor 45 Ti, Beckman). Proteins were  
230 separated on denaturing gels [46]. A mini-Protean III cell electrophoresis apparatus (Bio-Rad)  
231 was used in all cases. After migration, gels were either stained with Coomassie Blue R-250,  
232 enzymatic activities were revealed and proteins were detected with anti-H<sub>2</sub>ase antibodies.  
233 Protein bands were cut out from gels and stored at -20°C prior to mass spectrometry analysis.  
234 *Western Blotting*- Proteins were subjected to SDS gels and transferred to nitrocellulose  
235 membranes (Electran) with the Fast blot apparatus (Biometra) at 5 mA/cm<sup>2</sup> for 30 min. The  
236 blots were then processed and developed as previously described by Castelle et al. [47].  
237 Primary antibodies used were directed against H<sub>2</sub>ase from *A. aeolicus* or *Desulfovibrio*.  
238 Tryptic digestion of excised gel plugs, Ion Trap and MALDI-TOF mass spectrometry protein  
239 identification were performed, as previously described by Guiral et al. [46].  
240 *Data analysis*- Protein identification was done by the TurboSEQUENT algorithm (version 28,  
241 rev. 12) using the NCBI database (02/28/2006, <http://www.ncbi.nlm.nih.gov>) restricted to the  
242 *Clostridium* genus containing 498879 entries. The spectra were analyzed for searching for  
243 average peptide peaks (m/z 600 to 3500 Da). Search parameter criteria were set as follows:  
244 two missed cleavage sites accepted variable methionine oxidation, cysteine  
245 carbamidomethylation, 1.5 and 1.0 Da as maximum precursor and fragment tolerance. Protein  
246 identification was considered to have been obtained when at least 2 unique peptides in 2  
247 independent experiments were detected. In our analyses, some peptides matched with  
248 different H<sub>2</sub>ases from various strains. Only the strains displaying various identified proteins  
249 were accepted.  
250

251 **3. Results**

252

253 **3.1. Effect of carbohydrate type on overall hydrogen production performances**

254

255 During the course of the experiments, only H<sub>2</sub> and CO<sub>2</sub> were produced as gaseous products,  
256 with no detectable CH<sub>4</sub>, indicating that the heat pretreatment was effective in suppressing  
257 methanogen activity. The Gompertz model provided a good fit for the H<sub>2</sub> production data,  
258 with determination coefficients R<sup>2</sup> over 0.98 for all batch tests (Table 1).

259 The type of substrate had a significant effect on H<sub>2</sub> production performance (Table 1). Among  
260 different kinds of carbohydrates, fructose and glucose cultures gave the best H<sub>2</sub> production  
261 potentials (*P*) (2.31 and 2.24 L/L, respectively). These monosaccharide cultures were faster in  
262 reaching their peak of H<sub>2</sub> production than other disaccharide and trisaccharide cultures (7.7  
263 and 9.7 days, respectively). The highest yield (1.84 mol-H<sub>2</sub>/mol-hexose) was obtained with  
264 fructose and the lowest with maltotriose (1.38 mol-H<sub>2</sub>/mol-hexose), showing that the higher  
265 the substrate chain length, the lower the H<sub>2</sub> production yield. Indeed, a significant negative  
266 correlation was observed between the H<sub>2</sub> yield and the number of monomer units (Pearson's  
267 correlation coefficient  $r = -0.82$ ,  $p < 0.005$ ), indicating a negative impact from the hydrolysis  
268 step. Among disaccharide cultures, higher H<sub>2</sub> yields were observed from alpha-linked maltose  
269 cultures than beta-linked cellobiose cultures, suggesting an effect of the glycoside linkage  
270 type.

271 Whatever the substrate, the H<sub>2</sub> production phase was followed by a H<sub>2</sub> consumption phase  
272 (Figure 1). Indeed, the H<sub>2</sub> content in the gas phase increased until reaching between 31.0%  
273 and 34.2% at the *P* time; it then decreased to 22.7%-27.6% at the end of the experiments. The  
274 highest H<sub>2</sub> consumption rate (*R<sub>c</sub>*) was observed in the cellobiose cultures (Table1).

275 As expected, the pH decreased over time from 5.5 to 4.0 in average. The pH drop was faster  
276 for the most efficient monosaccharides cultures when compared to di- and tri-saccharides. A  
277 significant negative correlation was observed between pH and H<sub>2</sub> production (Pearson's  $r > -$   
278 0.97,  $p < 0.001$ ). However, no significant pH difference was observed using different  
279 carbohydrates at *P* time despite the difference in H<sub>2</sub> production and yield (final pH = 4.0 ±  
280 0.0) (Table 1). Moreover, no significant change in pH was observed during the H<sub>2</sub>  
281 consumption phase, despite the change in metabolic patterns (Table 2).

282

### 283 3.2. Effect of carbohydrate type on the fermentative routes

284

285 Different distributions of the metabolic products were observed depending on the substrate,  
286 although acetic and butyric acids were the major VFAs produced in all batch tests (Table 2).  
287 Indeed, after *P* was reached the acetate and butyrate molar content within the soluble  
288 microbial products ranged from 24.7% to 30.4% and from 58.0% to 69.7%, respectively. This  
289 result indicates that acetate-butyrate fermentation occurred whatever the substrate used. The  
290 highest acetate and butyrate levels were observed in sucrose cultures, where high *P* was  
291 obtained. The other byproducts corresponded to caproate, ethanol and lactate (1.5 - 2.7 %, 2.8  
292 - 10.5 % and 0 - 3.9%, respectively). Similar metabolic product distributions were observed in  
293 the monosaccharide cultures. In contrast, significant differences in metabolic profiles were  
294 obtained with the three different disaccharides: sucrose, cellobiose and maltose. The highest  
295 caproate, ethanol and lactate contents were obtained in the cellobiose cultures, a result which  
296 corroborates the negative influence of the beta-linkage type on H<sub>2</sub> production. When *P* was  
297 achieved, caproate production was only detected in the cellobiose-, maltose- and maltotriose  
298 cultures, where lower H<sub>2</sub> yields were obtained (Table 1). The least effective maltotriose  
299 culture was characterized by the highest concentrations of caproate, ethanol and lactate at *P*  
300 time (Table 2). Interestingly, and in total contrast to the maltotriose culture, the maltose

301 culture showed the lowest caproate, ethanol and lactate levels, indicating the effect of  
302 substrate chain length on the fermentation route. No correlation was observed between H<sub>2</sub>  
303 production performance and the ratio of butyrate to acetate concentrations (Bu/Ac) (Table 2)  
304 when *P* was reached (Pearson's  $r = 0.35$ ,  $p > 0.05$ ). At the final stage, a decrease in the Bu/Ac  
305 ratio was observed in all batch tests during the H<sub>2</sub> consumption phase (Table 1). Except for  
306 fructose culture, a significant decrease in butyrate concentrations was observed after 14-day  
307 incubation. Concomitantly, the caproate end product accumulated significantly in the  
308 disaccharide cultures, indicating that different metabolic pathways were being utilized at the  
309 end of the experiment.

310

### 311 **3.3. Effect of carbohydrate type on the hydrogen-producing bacterial populations**

312

313 Similar bacterial- and *Clostridium*-specific 16S rDNA CE-SSCP profiles were obtained  
314 during the 14 days of incubation, supporting the conclusion that clostridial species enriched  
315 by heat-shock pretreatment dominated the H<sub>2</sub>-producing mixed cultures (data not shown). In  
316 Figure 2, the *hydA* gene-based CE-SSCP profiles are presented for the *P* point reached. No  
317 significant change in the HPB population was observed between the *P* time and the end of the  
318 experiments despite the presence of the H<sub>2</sub>-consumption phase. The phylogenetic affiliation  
319 of the eight different *hydA* genes, the molecular markers of HPB, is illustrated in Figure 3.  
320 The retrieved sequences were related to various species among the *Clostridium* genus:  
321 *Clostridium acetobutylicum*, *Clostridium cellulolyticum*, *Clostridium kluyveri*, *Clostridium*  
322 *saccharobutylicum* and *Clostridium sporogenes*.

323 Overall, the type of carbohydrate had a significant effect on the HPB population structures  
324 (ANOSIM  $R = 0.85$ ,  $p < 0.005$ ). The fructose, glucose or sucrose cultures, which showed  
325 similar *P* values and fermentation end-products, displayed similar *hydA* CE-SSCP profiles  
326 (Figure 2). Peak 1 (70% identity with the HydA sequence of *C. sporogenes*) dominated the

327 CE-SSCP profiles of the glucose, fructose, sucrose and the cellobiose cultures. The HydA  
328 sequences corresponding to CE-SSCP peaks 2, 4 and 5 detected in the sucrose- and cellobiose  
329 cultures were related to that of *C. acetobutylicum* (86-88.6% identity). The cellobiose cultures  
330 displayed the highest Simpson's diversity index values ( $2.8 \pm 0.3$ ) compared to other cultures  
331 (ranging from 1.4 to 1.9). The HydA sequence from peak 3 was related to *C. cellulolyticum*  
332 (72.5% identity) which belongs to the *Clostridium* cluster III. The HydA sequence from peaks  
333 6 and 7 were affiliated, respectively, to those of *C. saccharobutylicum* (95.2% identity) and *C.*  
334 *kluuyveri* (79.4% identity). Finally, the CE-SSCP profiles of maltose and maltotriose cultures  
335 differed from those of other carbohydrate cultures by the predominance of another HydA  
336 sequence corresponding to peak 8 and related to *C. acetobutylicum* (87.5% identity).

337

#### 338 **3.4. Hydrogenase identification by metaproteomic approach**

339

340 No substantial difference in the total protein pattern was observed between the various  
341 substrate cultures **at the end of the experiments, assumed as the end of the H<sub>2</sub> consumption**  
342 **phase**. An example of total protein pattern is presented in Figure 4A. Various bands were  
343 labeled by the antibodies which confirmed the presence of various H<sub>2</sub>ases in the samples  
344 (Figure 4B). The major difference was observed between the cultures on cellobiose and those  
345 on the other substrates (e.g. glucose and fructose), in accordance with CE-SSCP data. The  
346 H<sub>2</sub>ases present in the fraction were precisely identified by proteomic analysis (Table 3). The  
347 H<sub>2</sub>ase-like proteins were related to those from the different species of the *Clostridium* genus:  
348 *Clostridium carboxidivorans*, *C. cellulolyticum*, *Clostridium novyi* and *C. sporogenes*. The  
349 proteins identified from glucose and fructose cultures were [FeFe]-H<sub>2</sub>ases and a subunit  
350 homologous to the [2Fe-2S] subunit from NADH dehydrogenase. In the cellobiose samples,  
351 [FeFe]-H<sub>2</sub>ase and the Ech H<sub>2</sub>ase (i.e. *E. coli* H<sub>2</sub>ase 3-type) subunit homologous to [NiFe]-



352 H<sub>2</sub>ase were identified (Table 3). From the membrane fraction of the cellobiose cultures,  
353 subunit membrane-bound complexes were identified as belonging to the Ech H<sub>2</sub>ase group,  
354 proposed as H<sub>2</sub>-producing [NiFe]-H<sub>2</sub>ases ([NiFe]-H<sub>2</sub>ase group 4, as defined by Vignais et al.  
355 [28, 48]).  
356

#### 357 4. Discussion

358

359 In this paper, a gradually increasing H<sub>2</sub> yield was observed from mesophilic clostridial mixed  
360 cultures depending on the chain length: fructose and glucose (monosaccharides) > sucrose,  
361 maltose and cellobiose (disaccharides) > maltotriose (trisaccharide). These results  
362 demonstrate that glycosidic hydrolysis was less adapted to efficient H<sub>2</sub> production. These  
363 findings are consistent with those obtained from mesophilic clostridial consortia isolated from  
364 riverbed sediments using different sugar sources [14]. In contrast, Ferchichi et al. [49] found  
365 that disaccharides (lactose, sucrose and maltose) produced twice as much H<sub>2</sub> as  
366 monosaccharides (glucose and fructose) using a pure culture of *Clostridium*  
367 *saccharoperbutylacetonicum* ATCC 27021. In addition, Yokoyama et al. [13] achieved  
368 similar H<sub>2</sub> yields (2.68-2.65 mol-H<sub>2</sub>/mol-hexose) from thermophilic anaerobic microflora  
369 using cellobiose and glucose as the substrate. The optimal type of substrate for H<sub>2</sub> production  
370 by our mesophilic mixed culture varied no doubt because of a different selection of clostridial  
371 HPB species. In this study, it is noteworthy that an effect of the glycoside linkage on H<sub>2</sub>  
372 production was shown by comparing cellobiose and maltose culture performances. A similar  
373 glycoside linkage effect with opposite results has already been reported in a  
374 hyperthermophilic pure culture of the archaeon *Pyrococcus furiosus* [50]. Chou et al. [50]  
375 proposed that different H<sub>2</sub> productions from cellobiose and maltose by *P. furiosus* were due to  
376 changes in metabolic routes. In our mixed cultures, the different H<sub>2</sub> yields can be explained  
377 by changes in both HPB population and metabolic routes.

378

379 To date, glucose has been the most commonly-used carbon source for determining H<sub>2</sub>  
380 production ability in laboratories. The H<sub>2</sub> yields obtained from our glucose cultures (1.79  
381 mol-H<sub>2</sub>/mol-hexose) were slightly higher than the reported yields of 1.46 mol-H<sub>2</sub>/mol-glucose

382 [51] and 1.67 mol-H<sub>2</sub>/mol-glucose [52] from comparable batch tests using mixed microbial  
383 cultures of heat-pretreated anaerobic sludge. In contrast, clostridial pure cultures, such as *C.*  
384 *acetobutylicum* [53] and *C. saccharoperbutylacetonicum* ATCC 13564 [54] exhibited higher  
385 H<sub>2</sub> yields (2.0 and 3.1 mol-H<sub>2</sub>/mol-glucose, respectively) than our clostridial mixed cultures.  
386 Using cellobiose as substrate, Ren et al. [55] also achieved higher H<sub>2</sub> yields in different pure  
387 cultures (e.g. *C. acetobutylicum* and *C. cellulolyticum*) compared to the yield in our mixed  
388 cultures: their results ranged from 1.6 to 2.3 mol-H<sub>2</sub>/mol-hexose, ours was 1.5 mol-H<sub>2</sub>/mol-  
389 hexose. Interestingly, *C. acetobutylicum* and *C. cellulolyticum* were detected in our cellobiose  
390 cultures (Figure 2 and 3). These results confirm that in general mixed cultures produce less H<sub>2</sub>  
391 than pure cultures with pure substrates. These results can be explained first of all by the  
392 operating conditions, which were probably not optimal for the growth of such recognized  
393 efficient HPB as *C. acetobutylicum*, *C. cellulolyticum* or *C. sporogenes*. An example here is  
394 the initial pH of our medium which was adjusted to 5.5. This is lower than the optimal pH of  
395 *Clostridium* species, even though this pH is known as optimal for H<sub>2</sub> production in mixed  
396 cultures. But the low H<sub>2</sub> yield from mixed cultures can be related to the presence of clostridial  
397 HCB and negative inter-species interaction occurring in complex anaerobic microbial  
398 communities. Such biotic interactions have already been observed in artificially-engineered  
399 fermentative ecosystems used in cheese ripening [56].

400

401 The variations in H<sub>2</sub> production performance were associated with changes in metabolic  
402 profiles and HPB populations. The more efficient HPB cultures dominated by *C. sporogenes*  
403 were characterized by high levels of acetate and butyrate production, each with pathways  
404 linked to H<sub>2</sub> production; and, simultaneously, by low ethanol and lactate yields, as alternative  
405 but non-H<sub>2</sub>-producing routes. Indeed, clostridial species are usually known to produce H<sub>2</sub>  
406 from a wide variety of carbohydrates *via* the butyrate-acetate fermentation route [2]. More

407 precisely, *C. sporogenes* is known to ferment mainly amino acids [57]. Recently, the  
408 consumption of H<sub>2</sub> produced by glucose- or starch- fed HPB cultures amended by peptone has  
409 been associated with the presence of *C. sporogenes* [58]. In glucose or maltotriose cultures,  
410 H<sub>2</sub> consumption was concomitant with an increase in acetate. Consequently, H<sub>2</sub> consumption  
411 detected in our cultures was most probably due to homoacetogenesis: it is a favored reaction  
412 at pH 5.5 producing only acetate from H<sub>2</sub> and CO<sub>2</sub> [59]. In the disaccharide cultures, H<sub>2</sub>  
413 consumption probably also resulted from caproate formation [10, 60]. Indeed, the increase in  
414 caproate concentration between the *P* and the final stages was associated with decreases in  
415 concentrations of butyrate, CO<sub>2</sub> and H<sub>2</sub>. These findings are in agreement with another  
416 pathway for caproate formation using sucrose as the substrate in fermentative HPB mixed  
417 cultures. These cultures consumed equimolar butyrate, H<sub>2</sub> and CO<sub>2</sub> in a thermodynamically-  
418 favorable reaction ( $\Delta G = -143.34$  kJ) [60]. Interestingly, previous studies on *C. kluyveri* during  
419 H<sub>2</sub>-producing glucose fermentation have reported the possibility of caproate formation from  
420 ethanol and acetate or ethanol and butyrate [61].

421

422 The changes in HPB population structure associated with variations in the H<sub>2</sub> yield as a  
423 function of the different carbohydrates was particularly interesting because each pure  
424 clostridial culture was reported as metabolizing each of the six substrates tested [62].  
425 Although glucose is the preferred carbohydrate of many clostridial species, such species have  
426 metabolic resources flexible enough to ferment a wide range of carbohydrates [12]. For  
427 instance, *C. acetobutylicum* can metabolize glucose, cellobiose and maltose [55, 62]. Thus the  
428 variation in H<sub>2</sub> yields may be due entirely to the use of different mechanisms for the  
429 hydrolysis of the glycoside linkage and transport [12]. In this study, however, the structure of  
430 the HPB populations changed depending on the type of the glycoside linkage and the chain  
431 length. A single dominant HPB, i.e. *C. sporogenes* was selected in glucose, fructose and

432 sucrose cultures, cultures which presented the highest H<sub>2</sub> yield and similar metabolic profiles.  
433 It is noteworthy that *C. sporogenes* has been reported previously as the dominant, key HPB  
434 species in mesophilic mixed cultures using glucose or sucrose as the substrate [16, 58, 63].  
435 However, different HPB populations established on cellobiose, maltose and maltotriose have  
436 been associated with different metabolic profiles. Remarkably, a more diverse HPB  
437 population made up of *C. sporogenes*, *C. cellulolyticum*, *C. acetobutylicum*, *C.*  
438 *saccharobutylicum* and *C. kluyveri* emerged with cellobiose as the substrate. The use of beta-  
439 linked carbohydrates for H<sub>2</sub> production by mesophilic mixed cultures seems to require a wider  
440 range of clostridial species. These results suggest that cooperation between HPB can be  
441 obtained on beta-linked carbohydrates whereas competition seems to occur on unlinked and  
442 alpha-linked carbohydrates. *C. acetobutylicum* and *C. cellulolyticum* have been previously  
443 reported as efficient H<sub>2</sub> producers on cellobiose [55, 64]. Like other clostridial species, *C.*  
444 *saccharobutylicum* is able to grow on a wide range of carbohydrates, including cellobiose  
445 [62]. *C. kluyveri* can grow anaerobically with ethanol and acetate as its sole source of energy  
446 [65]. Interestingly, extreme thermophilic anaerobic microflora displayed less diversity of 16S  
447 rRNA genes when enriched by cellobiose rather than glucose [13]. Yokoyama et al. [13]  
448 enriched fairly similar microbial communities whatever the type of hexose while a clearly  
449 different microbial community was enriched on xylose. Significant difference between  
450 microbial communities grown on glucose or xylose have also been observed previously in  
451 fermentative mixed cultures [19]. In our study, changes in dominant HPB species were  
452 observed only when using different hexose-based carbohydrates. Overall, these findings  
453 indicate firstly that clostridial HPB structure is sensitive to substrate change and secondly that  
454 a specialization of the clostridial population occurs depending on the characteristics of the  
455 carbohydrate used with mixed cultures. Shifts in the dominant HPB species associated with  
456 variations in the H<sub>2</sub> yield have already been observed in batch experiments run at different

457 temperatures [16]. Moreover, as observed in cellobiose cultures, the increase in *hydA* gene  
458 diversity was also detected in previous experiments with higher pH [10]. In this study,  
459 changes in both diversity and the dominant HPB were observed depending on the type of  
460 carbohydrate.

461

462 Using the metaproteomic approach, various proteins associated with clostridial species were  
463 identified from mixed cultures. From glucose or fructose cultures at least two different  
464 [FeFe]-H<sub>2</sub>ases with different molecular mass were detected in the soluble fraction. Recently,  
465 Calusinska et al. [66], on the basis of genome analysis, pointed out that some clostridial  
466 species contain numerous distinct [FeFe]-H<sub>2</sub>ases presumably to allow them to adapt quickly  
467 to changing conditions. The species identified in glucose and fructose substrates are linked to  
468 [FeFe]-H<sub>2</sub>ases from *C. novyi*, *C. carboxidivorans* and *C. sporogenes*. These clostridial  
469 species present various [FeFe]-H<sub>2</sub>ases belonging to the group A6, B2 and B3 [66]. Using the  
470 metaproteomic approach, [FeFe]-H<sub>2</sub>ases similar to those belonging to B2 and B3 types were  
471 clearly identified. A protein belonging to the NADH dehydrogenase family was also  
472 identified in the soluble fraction (Figure 4B, band d). This protein is similar to [2Fe2S]  
473 ferredoxin. Analysis of the genome context showed that the corresponding genes belonged to,  
474 respectively, an operon encoding the [FeFe]-H<sub>2</sub>ase and the NADH quinone dehydrogenase.  
475 The NADH subunit identified belonged to the group A8. This latter group seemed to be  
476 NAD-dependent and was proposed as “heterodimeric bifurcative” H<sub>2</sub>ase [66]. However as the  
477 other subunits were not identified, we cannot affirm that this enzyme was present in our  
478 conditions. Using cellobiose as the substrate, only one [FeFe]-H<sub>2</sub>ase was detected similar to  
479 that from *C. cellulolyticum* (group A1). A second H<sub>2</sub>ase was identified in both the soluble as  
480 well membrane fractions. This subunit belongs to the [NiFe]-H<sub>2</sub>ase family. Analysis of the  
481 genome showed that it was located in an operon with at least three other genes similar to Ech

482 H<sub>2</sub>ases. This enzyme is similar to the [NiFe]-H<sub>2</sub>ases belonging to the group 4 defined by  
483 Vignais et al. [28, 48] and was closely related to the NADH:ubiquinone oxidoreductase. This  
484 enzyme has been identified in various *Bacteria* and *Archaea* and its presence in *Clostridia* has  
485 been the subject of speculation on the basis of genome analysis only: there is no data  
486 concerning the function of this enzyme in *Clostridia*. In methanogens, it plays a role in the  
487 first stage of methanogenesis. In *Desulfovibrionaceae* family, Ech H<sub>2</sub>ase can work  
488 bidirectionally, depending on the growth conditions [67]. This amounts to the first  
489 identification of this group of H<sub>2</sub>ase in *Clostridia*. [NiFe]-H<sub>2</sub>ases belonging to group 1  
490 (defined by Vignais et al. [28, 48]) was not detected in this study. These [NiFe]-H<sub>2</sub>ases are  
491 usually involved in H<sub>2</sub> uptake linked with energy metabolism and to our knowledge have only  
492 been detected in the clostridial genome by sequence homology. Their physiological roles as  
493 well as their protein properties in clostridial species are unknown.

494

495 Both the genetic and proteomic analyses highlighted changes in H<sub>2</sub>ases diversity associated  
496 with changes in carbohydrate type and, thus, H<sub>2</sub> production performances. Changes in genetic  
497 diversity in [FeFe]-H<sub>2</sub>ases have been previously demonstrated in relation to H<sub>2</sub> production  
498 performances [15, 20]. Proteomic shifts have also been associated with metabolic shifts  
499 during fermentation carried out by clostridial species [22, 23]. [FeFe]-H<sub>2</sub>ases sequences from  
500 similar clostridial species were recovered from the H<sub>2</sub>-producing mixed cultures by these two  
501 different molecular approaches. Like other primers currently cited in the literature and  
502 targeting the cluster H of the *hydA* genes, the primers used in this study were only able to  
503 target the sequences of Group A of [FeFe]-H<sub>2</sub>ases, as defined by Calusinska et al. [66].  
504 Consequently, the [FeFe]-H<sub>2</sub>ases belonging to group B, which were highlighted by the  
505 proteomic approach and thus assumed to be active in the cultures, could not be detected by  
506 the genetic fingerprinting method. Even so, it is important to emphasize that the *hydA* CE-

507 SSCP method has been proven helpful in providing an overview of HPB diversity and  
508 structure in numerous samples from dark fermentation bioreactors. It is also useful in  
509 comparing variations in such diversity and structure in response to changes in environmental  
510 parameters [10, 16]. Using proteomic techniques, [Ni-Fe]-H<sub>2</sub>ases were detected in cellobiose  
511 cultures, cultures which showed the highest H<sub>2</sub> consumption rates. Recently, plasmid or  
512 chromosomal genes encoding [NiFe]-H<sub>2</sub>ases have been detected in the genome of some  
513 members of the *Clostridium* genus such as *C. acetobutylicum*, *C. cellulolyticum* or *C.*  
514 *sporogenes* [66]. Interestingly, as found in this study, these clostridial strains were detected  
515 during the H<sub>2</sub> consumption phase of previous batch experiments carried out in our laboratory  
516 [10]. Contrary to [FeFe]-H<sub>2</sub>ases and [NiFe]-H<sub>2</sub>ases from *Proteobacteria*, [NiFe]-H<sub>2</sub>ases from  
517 *Clostridia* have not yet been studied and their physiological functions are still unknown [66].  
518 Consequently, it is still unclear whether clostridial [NiFe]-H<sub>2</sub>ases can be associated with H<sub>2</sub>  
519 consumption in dark fermentation bioreactors. Further research is needed to determine the  
520 physiological roles played by the different [Fe-Fe]- and [Ni-Fe]-H<sub>2</sub>ases in clostridial species.  
521 To further analyze the role of these enzymes, differential transcriptome analyses of H<sub>2</sub>ase-  
522 encoding genes under different operating conditions could well provide the basis for future  
523 work.

524



## 525 **5. Conclusions**

526

527 The characteristics of carbohydrates were found to be important criteria influencing the  
528 performance of dark fermentation systems. The hydrolysis of carbohydrate was shown as a  
529 critical step in the H<sub>2</sub> production pathway. Monosaccharides led to more efficient H<sub>2</sub>  
530 production performances when compared to di- and tri-saccharides. Moreover, the negative  
531 effect of the glycoside chain length was amplified by the glycoside beta-linkage type. The  
532 difference in performance with various carbohydrates was related to the enrichment of  
533 different specialized clostridial species, which used diverse metabolic routes. Finally, we have  
534 expanded the diversity spectrum of clostridial H<sub>2</sub>ases potentially involved in H<sub>2</sub> metabolism  
535 in fermentative mixed cultures by using a combination of proteomic and molecular genetic  
536 approaches. Future work will undertake to continue clarifying the function of these diverse  
537 H<sub>2</sub>ases in clostridial species and to identify the key regulatory pathways in engineered/natural  
538 H<sub>2</sub>-producing ecosystems.

539 **Acknowledgements**

540

541 We gratefully acknowledge the financial support from the ‘Institut National de la Recherche  
542 Agronomique’ (INRA) through a postdoctoral fellowship. This work was funded by the  
543 InGEcoH Project from the French National Research Agency (ANR) (ANR contract number  
544 2008-BIOE-005-01). We also gratefully acknowledge the contribution of Pacale Infossi (BIP)  
545 for technical assistance and Sabrina Lignon and Régine Lebrun (Proteomic Analysis Center,  
546 IFR88, CNRS, Marseille) for proteomic analysis. BIP was financially supported by the  
547 CNRS, the Région-Provence-Alpes Côte d’Azur and Marseille Metropole. We thank Tim  
548 Sparham for revising the English of the manuscript. We would like to thank the reviewers for  
549 her/his comments that help us to improve the quality of our paper.

550 **References**

551

552 [1] Hawkes FR, Dinsdale R, Hawkes DL, Hussy I. Sustainable fermentative hydrogen  
553 production: challenges for process optimisation. *Int J Hydrogen Energy* 2002;27(11-  
554 12):1339-47.

555 [2] Hawkes FR, Hussy I, Kyazze G, Dinsdale R, Hawkes DL. Continuous dark  
556 fermentative hydrogen production by mesophilic microflora: Principles and progress.  
557 *Int J Hydrogen Energy* 2007;32(2):172-84.

558 [3] Guo XM, Trably E, Latrille E, Carrere H, Steyer JP. Hydrogen production from  
559 agricultural waste by dark fermentation: A review. *Int J Hydrogen Energy*  
560 35(19):10660-73.

561 [4] Shin HS, Youn JH, Kim SH. Hydrogen production from food waste in anaerobic  
562 mesophilic and thermophilic acidogenesis. *Int J Hydrogen Energy* 2004;29(13):1355-  
563 63.

564 [5] Chong ML, Sabaratnam V, Shirai Y, Hassan MA. Biohydrogen production from  
565 biomass and industrial wastes by dark fermentation. *Int J Hydrogen Energy*  
566 2009;34(8):3277-87.

567 [6] Kraemer JT, Bagley DM. Improving the yield from fermentative hydrogen production.  
568 *Biotechnol Lett* 2007;29(5):685-95.

569 [7] Aceves-Lara CA, Latrille E, Steyer JP. Optimal control of hydrogen production in a  
570 continuous anaerobic fermentation bioreactor. *Int J Hydrogen Energy*  
571 2010;35(19):10710-8.

572 [8] Li CL, Fang HHP. Fermentative hydrogen production from wastewater and solid  
573 wastes by mixed cultures. *Crit Rev Environ Sci Tech* 2007;37(1):1-39.

574 [9] Wang JL, Wan W. Factors influencing fermentative hydrogen production: A review.  
575 *Int J Hydrogen Energy* 2009;34(2):799-811.

- 576 [10] Quéméneur M, Hamelin J, Latrille E, Steyer J-P, Trably E. Functional versus  
577 phylogenetic fingerprint analyses for monitoring hydrogen-producing bacterial  
578 populations in dark fermentation cultures. *Int J Hydrogen Energy* 2011;36(6):3870-9.
- 579 [11] Mitchell WJ. Carbohydrate uptake and utilization by *Clostridium beijerinckii* NCIMB  
580 8052. *Anaerobe* 1996;2(6):379-84.
- 581 [12] Servinsky MD, Kiel JT, Dupuy NF, Sund CJ. Transcriptional analysis of differential  
582 carbohydrate utilization by *Clostridium acetobutylicum*. *Microbiology*  
583 2010;156:3478-91.
- 584 [13] Yokoyama H, Moriya N, Ohmori H, Waki M, Ogino A, Tanaka Y. Community  
585 analysis of hydrogen-producing extreme thermophilic anaerobic microflora enriched  
586 from cow manure with five substrates. *Appl Microbiol Biotechnol* 2007;77(1):213-22.
- 587 [14] Singh S, Sudhakaran AK, Sarma PM, Subudhi S, Mandal AK, Gandham G, Lal B.  
588 Dark fermentative biohydrogen production by mesophilic bacterial consortia isolated  
589 from riverbed sediments. *Int J Hydrogen Energy* 2010;35(19):10645-52.
- 590 [15] Huang Y, Zong WM, Yan X, Wang RF, Hemme CL, Zhou JZ, Zhou ZH. Succession  
591 of the bacterial community and dynamics of hydrogen producers in a hydrogen-  
592 producing bioreactor. *Appl Environ Microbiol* 2010;76(10):3387-90.
- 593 [16] Quéméneur M, Hamelin J, Latrille E, Steyer J-P, Trably E. Development and  
594 application of a functional CE-SSCP fingerprinting method based on [Fe-Fe]-  
595 hydrogenase genes for monitoring hydrogen-producing *Clostridium* in mixed cultures.  
596 *Int J Hydrogen Energy* 2010;35(24):13158-67.
- 597 [17] Wang X, Hoefel D, Saint CP, Monis PT, Jin B. The isolation and microbial  
598 community analysis of hydrogen producing bacteria from activated sludge. *J Appl*  
599 *Microbiol* 2007;103(5):1415-23.

- 600 [18] Iyer P, Bruns MA, Zhang HS, Van Ginkel S, Logan BE. H<sub>2</sub>-producing bacterial  
601 communities from a heat-treated soil inoculum. *Appl Microbiol Biotechnol*  
602 2004;66(2):166-73.
- 603 [19] Temudo MF, Muyzer G, Kleerebezem R, van Loosdrecht MCM. Diversity of  
604 microbial communities in open mixed culture fermentations: impact of the pH and  
605 carbon source. *Appl Microbiol Biotechnol* 2008;80(6):1121-30.
- 606 [20] Xing DF, Ren NQ, Rittmann BE. Genetic diversity of hydrogen-producing bacteria in  
607 an acidophilic ethanol-H<sub>2</sub>-coproducing system, analyzed using the Fe<sup>-</sup>-hydrogenase  
608 gene. *Appl Environ Microbiol* 2008;74(4):1232-9.
- 609 [21] Jo JH, Jeon CO, Lee DS, Park JM. Process stability and microbial community  
610 structure in anaerobic hydrogen-producing microflora from food waste containing  
611 kimchi. *J Biotechnol* 2007;131(3):300-8.
- 612 [22] Janssen H, Doring C, Ehrenreich A, Voigt B, Hecker M, Bahl H, Fischer RJ. A  
613 proteomic and transcriptional view of acidogenic and solventogenic steady-state cells  
614 of *Clostridium acetobutylicum* in a chemostat culture. *Appl Microbiol Biotechnol*  
615 2010;87(6):2209-26.
- 616 [23] Schaffer S, Isci N, Zickner B, Durre P. Changes in protein synthesis and identification  
617 of proteins specifically induced during solventogenesis in *Clostridium acetobutylicum*.  
618 *Electrophoresis* 2002;23(1):110-21.
- 619 [24] Stackebrandt E, Kramer I, Swiderski J, Hippe H. Phylogenetic basis for a taxonomic  
620 dissection of the genus *Clostridium*. *FEMS Immunol Med Microbiol* 1999;24(3):253-  
621 8.
- 622 [25] Collins MD, Lawson PA, Willems A, Cordoba JJ, Fernandezgarayzabal J, Garcia P,  
623 Cai J, Hippe H, Farrow JAE. The Phylogeny of the Genus *Clostridium* - Proposal of 5

- 624 New Genera and 11 New Species Combinations. *Int J Syst Bacteriol* 1994;44(4):812-  
625 26.
- 626 [26] Schmidt O, Drake HL, Horn MA. Hitherto unknown [Fe-Fe]-hydrogenase gene  
627 diversity in anaerobes and anoxic enrichments from a moderately acidic fen. *Appl*  
628 *Environ Microbiol* 2010;76(6):2027-31.
- 629 [27] Hung CH, Cheng CH, Cheng LH, Liang CM, Lin CY. Application of *Clostridium*-  
630 specific PCR primers on the analysis of dark fermentation hydrogen-producing  
631 bacterial community. *Int J Hydrogen Energy* 2008;33(5):1586-92.
- 632 [28] Vignais PM, Billoud B. Occurrence, classification, and biological function of  
633 hydrogenases: An overview. *Chem Rev* 2007;107(10):4206-72.
- 634 [29] Tolvanen KES, Santala VP, Karp MT. [FeFe]-hydrogenase gene quantification and  
635 melting curve analysis from hydrogen-fermenting bioreactor samples. *Int J Hydrogen*  
636 *Energy* 2010;35(8):3433-9.
- 637 [30] Tolvanen KES, Koskinen PEP, Ylikoski AI, Ollikka PK, Hemmila IA, Puhakka JA,  
638 Karp M. Quantitative monitoring of a hydrogen-producing *Clostridium butyricum*  
639 strain from a continuous-flow, mixed culture bioreactor employing real-time PCR. *Int*  
640 *J Hydrogen Energy* 2008;33(2):542-9.
- 641 [31] Delbes C, Moletta R, Godon JJ. Bacterial and archaeal 16S rDNA and 16S rRNA  
642 dynamics during an acetate crisis in an anaerobic digester ecosystem. *FEMS*  
643 *Microbiol Ecol* 2001;35(1):19-26.
- 644 [32] Lee DH, Zo YG, Kim SJ. Nonradioactive method to study genetic profiles of natural  
645 bacterial communities by PCR-single-strand-conformation polymorphism. *Appl*  
646 *Environ Microbiol* 1996;62(9):3112-20.

- 647 [33] Van Dyke MI, McCarthy AJ. Molecular biological detection and characterization of  
648 *Clostridium* populations in municipal landfill sites. *Appl Environ Microbiol*  
649 2002;68(4):2049-53.
- 650 [34] Peu P, Brugere H, Pourcher AM, Kerouredan M, Godon JJ, Delgenes JP, Dabert P.  
651 Dynamics of a pig slurry microbial community during anaerobic storage and  
652 management. *Appl Environ Microbiol* 2006;72(5):3578-85.
- 653 [35] Michelland RJ, Dejean S, Combes S, Fortun-Lamothe L, Cauquil L. StatFingerprints:  
654 a friendly graphical interface program for processing and analysis of microbial  
655 fingerprint profiles. *Mol Ecol Resour* 2009;9(5):1359-63.
- 656 [36] Team RDC. R: A language and environment for statistical computing. R Foundation  
657 for Statistical Computing, Vienna, Austria. 2009.
- 658 [37] Fromin N, Hamelin J, Tarnawski S, Roesti D, Jourdain-Miserez K, Forestier N,  
659 Teyssier-Cuvelle S, Gillet F, Aragno M, Rossi P. Statistical analysis of denaturing gel  
660 electrophoresis (DGE) fingerprinting patterns. *Environ Microbiol* 2002;4(11):634-43.
- 661 [38] Clarke KR. Nonparametric multivariate analyses of changes in community structure.  
662 *Aust J Ecol* 1993;18(1):117-43.
- 663 [39] Simpson EH. Measurement of diversity. *Nature* 1949;163:688.
- 664 [40] Thompson JD, D. G. Higgins, and T. J. Gibson. CLUSTAL W: improving the  
665 sensitivity of progressive multiple sequence alignment through sequence weighting,  
666 position-specific gap penalties and weight matrix choice. *Nucleic Acids Res*  
667 1994;22:4673-80.
- 668 [41] Hall T. BioEdit: a user-friendly biological sequence alignment editor and analysis  
669 program for Windows 95/98/NT. *Nucleic Acids Symp Ser* 1999;41:95-8.
- 670 [42] Kimura M. A simple method for estimating evolutionary rates of base substitutions  
671 through comparative studies of nucleotide sequence. *J Mol Biol* 1980;16:111-20.

- 672 [43] Saitou N, and M. Nei. The neighbor-joining method: a new method for reconstructing  
673 phylogenetic trees. *Mol Biol Evol* 1987;4:406-25.
- 674 [44] Felsenstein J. Confidence-Limits on Phylogenies - an Approach Using the Bootstrap.  
675 *Evolution* 1985;39(4):783-91.
- 676 [45] Gouy M, Guindon S, Gascuel O. SeaView Version 4: A Multiplatform Graphical User  
677 Interface for Sequence Alignment and Phylogenetic Tree Building. *Mol Biol Evol*  
678 27(2):221-4.
- 679 [46] Guiral M, Prunetti L, Lignon S, Lebrun R, Moinier D, Giudici-Orticoni MT. New  
680 insights into the respiratory chains of the chemolithoautotrophic and  
681 hyperthermophilic bacterium *Aquifex aeolicus*. *J Proteome Res* 2009;8(4):1717-30.
- 682 [47] Castelle C, Guiral M, Malarte G, Ledgham F, Leroy G, Brugna M, Giudici-Orticoni  
683 MT. A new iron-oxidizing/O<sub>2</sub>-reducing supercomplex spanning both inner and outer  
684 membranes, isolated from the extreme acidophile *Acidithiobacillus ferrooxidans*. *J*  
685 *Biol Chem* 2008;283(38):25803-11.
- 686 [48] Vignais PM, Billoud B, Meyer J. Classification and phylogeny of hydrogenases.  
687 *FEMS Microbiol Rev* 2001;25(4):455-501.
- 688 [49] Ferchichi M, Crabbe E, Hintz W, Gil GH, Almadidy A. Influence of culture  
689 parameters on biological hydrogen production by *Clostridium*  
690 *saccharoperbutylaceticum* ATCC 27021. *World J Microbiol Biotechnol* 2005;21(6-  
691 7):855-62.
- 692 [50] Chou CJ, Shockley KR, Connors SB, Lewis DL, Comfort DA, Adams MWW, Kelly  
693 RM. Impact of substrate glycoside linkage. and elemental sulfur on bioenergetics, of  
694 and hydrogen production by the hyperthermophilic Archaeon *Pyrococcus furiosus*.  
695 *Appl Environ Microbiol* 2007;73(21):6842-53.



- 696 [51] Davila-Vazquez G, Alatrisme-Mondragon F, de Leon-Rodriguez A, Razo-Flores E.  
697 Fermentative hydrogen production in batch experiments using lactose, cheese whey  
698 and glucose: influence of initial substrate concentration and pH. *Int J Hydrogen*  
699 *Energy* 2008;33(19):4989-97.
- 700 [52] Mu Y, Zheng XJ, Yu HQ, Zhu RF. Biological hydrogen production by anaerobic  
701 sludge at various temperatures. *Int J Hydrogen Energy* 2006;31(6):780-5.
- 702 [53] Chin HL, Chen ZS, Chou CP. Fedbatch operation using *Clostridium acetobutylicum*  
703 suspension culture as biocatalyst for enhancing hydrogen production. *Biotechnol*  
704 *Progr* 2003;19(2):383-8.
- 705 [54] Alalayah WM, Kalil MS, Kadhum AAH, Jahim JM, Alauj NM. Hydrogen production  
706 using *Clostridium saccharoperbutylacetonicum* N1-4 (ATCC 13564). *Int J Hydrogen*  
707 *Energy* 2008;33(24):7392-6.
- 708 [55] Ren Z, Ward TE, Logan BE, Regan JM. Characterization of the cellulolytic and  
709 hydrogen-producing activities of six mesophilic *Clostridium* species. *J Appl Microbiol*  
710 2007;103(6):2258-66.
- 711 [56] Mounier J, Monnet C, Vallaeyts T, Arditi R, Sarthou AS, Helias A, Irlinger F.  
712 Microbial interactions within a cheese microbial community. *Appl Environ Microbiol*  
713 2008;74(1):172-81.
- 714 [57] Allison C, Macfarlane GT. Physiological and nutritional determinants of protease  
715 secretion by *Clostridium sporogenes*: characterization of six extracellular proteases.  
716 *Appl Microbiol Biotechnol* 1992;37:152-9.
- 717 [58] Li SL, Whang LM, Chao YC, Wang YH, Wang YF, Hsiao CJ, Tseng IC, Bai MD,  
718 Cheng SS. Effects of hydraulic retention time on anaerobic hydrogenation  
719 performance and microbial ecology of bioreactors fed with glucose-peptone and  
720 starch-peptone. *Int J Hydrogen Energy* 35(1):61-70.

- 721 [59] Chen AC, Ohashi A, Harada H. Acetate synthesis from H<sub>2</sub>/CO<sub>2</sub> in simulated and  
722 actual landfill samples. *Environ Technol* 2003;24(4):435-43.
- 723 [60] Yu HQ, Mu Y. Biological hydrogen production in a UASB reactor with granules. II:  
724 Reactor performance in 3-year operation. *Biotechnol Bioeng* 2006;94(5):988-95.
- 725 [61] Ding HB, Tan GYA, Wang JY. Caproate formation in mixed-culture fermentative  
726 hydrogen production. *Bioresource Technol* 101(24):9550-9.
- 727 [62] Keis S, Shaheen R, Jones DT. Emended descriptions of *Clostridium acetobutylicum*  
728 and *Clostridium beijerinckii*, and descriptions of *Clostridium*  
729 *saccharoperbutylaceticum* sp. nov. and *Clostridium saccharobutylicum* sp. nov. *Int*  
730 *J Syst Evol Microbiol* 2001;51:2095-103.
- 731 [63] Duangmanee T, Padmasiri SI, Simmons JJ, Raskin L, Sung S. Hydrogen production  
732 by anaerobic microbial communities exposed to repeated heat treatments. *Water*  
733 *Environ Res* 2007;79(9):975-83.
- 734 [64] Petitdemange E, Caillet F, Giallo J, Gaudin C. *Clostridium cellulolyticum* sp. nov., a  
735 cellulolytic, mesophilic species from decayed grass. *Int J Syst Bacteriol*  
736 1984;34(2):155-9.
- 737 [65] Seedorf H, Fricke WF, Veith B, Bruggemann H, Liesegang H, Strittmatter A,  
738 Miethke M, Buckel W, Hinderberger J, Li FL, Hagemeyer C, Thauer RK, Gottschalk  
739 G. The genome of *Clostridium kluyveri*, a strict anaerobe with unique metabolic  
740 features. *P Natl Acad Sci USA* 2008;105(6):2128-33.
- 741 [66] Calusinska M, Happe T, Joris B, Wilmotte A. The surprising diversity of clostridial  
742 hydrogenases: a comparative genomic perspective. *Microbiology* 2010;156:1575-88.
- 743 [67] Pereira PM, He Q, Valente FMA, Xavier AV, Zhou JZ, Pereira IAC, Louro RO.  
744 Energy metabolism in *Desulfovibrio vulgaris* Hildenborough: insights from  
745 transcriptome analysis. *Ant Leeuw Int J G* 2008;93(4):347-62.
- 746

747 **Captions to figures**

748

749 **Figure 1.** Representative dynamics of H<sub>2</sub> production from a mixed culture cultivated with  
750 fructose as substrate and heat-treated anaerobic digested sludge as inoculum. Experimental  
751 data (triangles) and predicted Gompertz equation (solid lines) are shown. The estimated  
752 values of  $P$ ,  $R_m$  and  $\lambda$  correspond to the H<sub>2</sub> production potential (mL/L), the maximum H<sub>2</sub>  
753 production rate (mL/L/day) and the lag-phase time (day), respectively. The  $R_c$  value,  
754 estimated by the H<sub>2</sub> decrease experimentally measured between the  $P$  time and the end of the  
755 experiments, corresponds to the H<sub>2</sub> consumption rate.

756

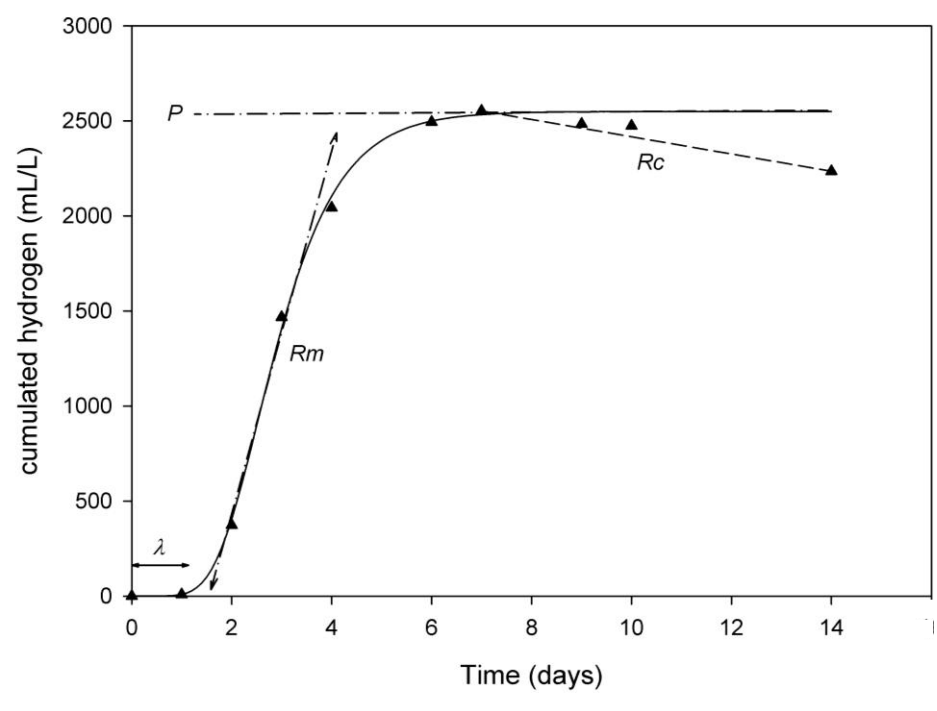
757 **Figure 2.** CE-SSCP profiles of *hydA* gene fragments retrieved from H<sub>2</sub>-producing  
758 experiments conducted from different carbohydrates, at maximum H<sub>2</sub> production yields. The  
759 different CE-SSCP profiles were aligned on the basis of the common ROX internal standard,  
760 and areas normalized. The x and y axis of each CE-SSCP profile represent, respectively, the  
761 relative peak migration distance and the relative peak intensity. A representative CE-SSCP  
762 profile from the three replicates is presented for each substrate. The dominant peaks of each  
763 CE-SSCP profile are marked with a number. The phylogenetic affiliation of the sequenced  
764 clones that match a numbered peak is given in Figure 3.

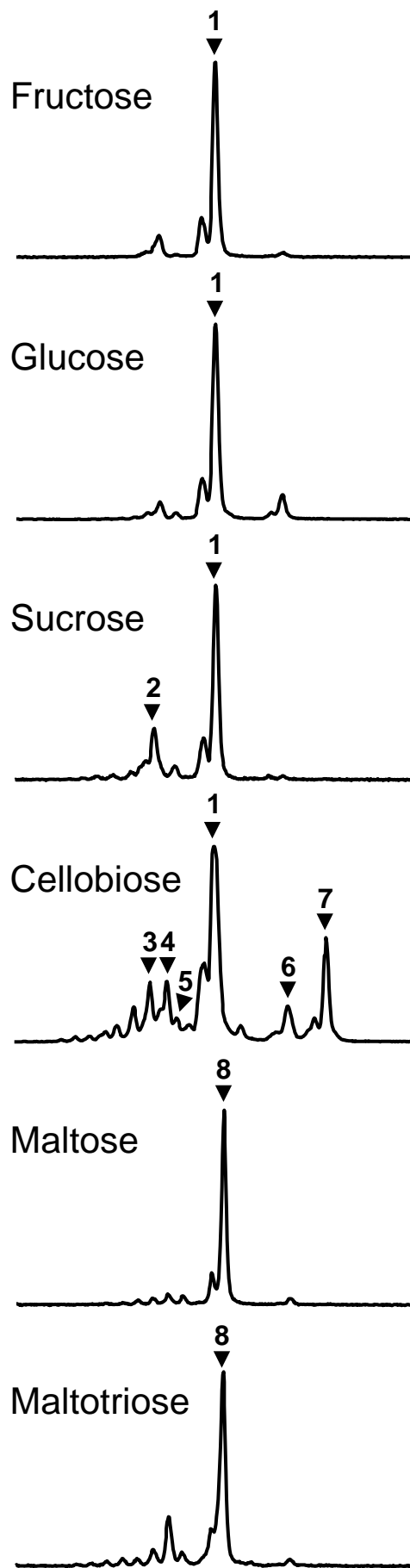
765

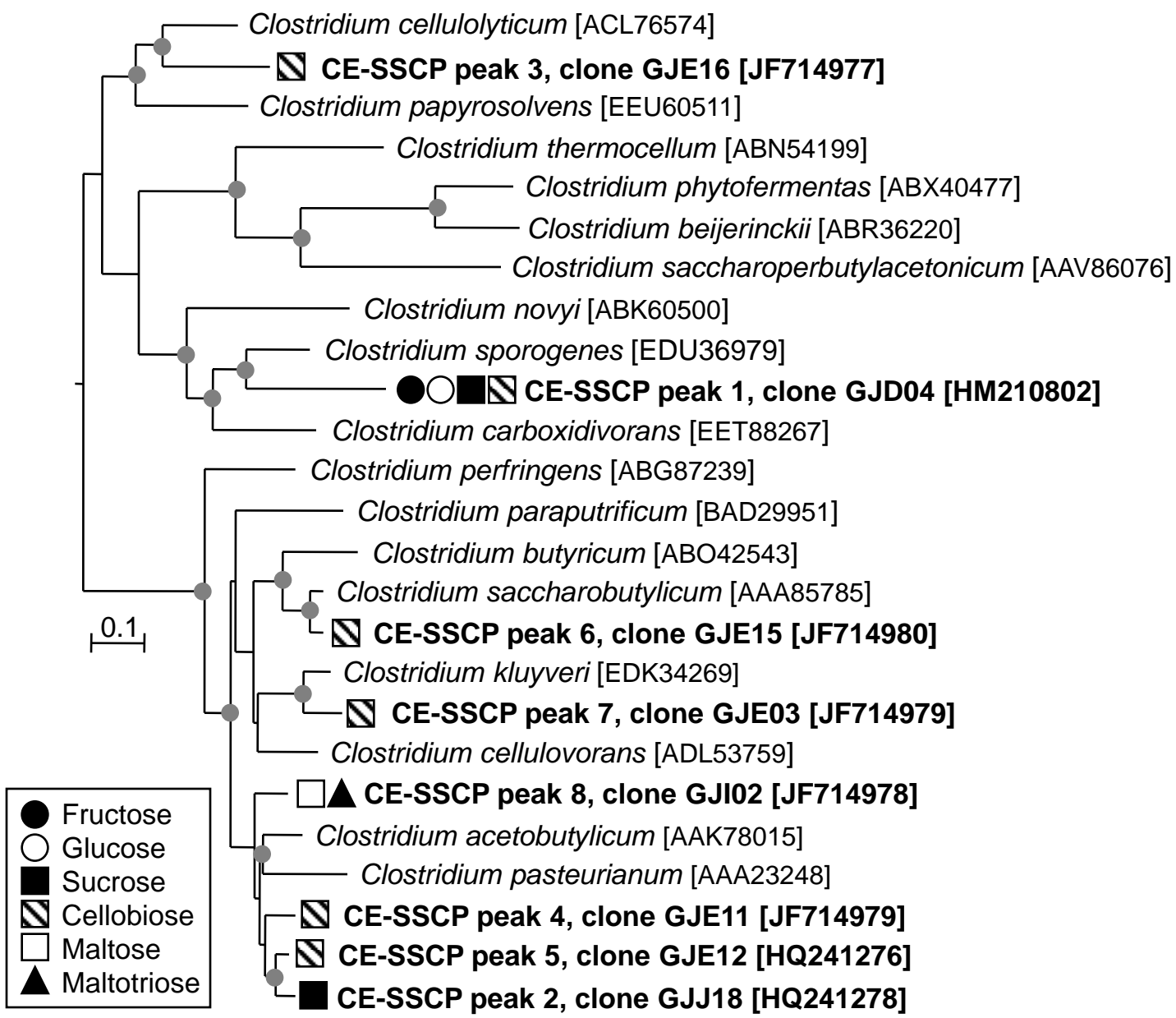
766 **Figure 3.** Neighbor-joining phylogenetic tree of the HydA sequences (134 amino acids). The  
767 Genbank accession numbers (in brackets) were obtained from the protein sequence databases.  
768 The sequences obtained in this study are in bold and highlighted. Bootstrap values ( $n = 1000$   
769 replicates) are indicated as grey circles (<50%). The scale bar indicates 5% sequence  
770 divergence. The *Desulfovibrio* HydA sequences (AAS96246, AAA23373 and CAA72423)  
771 were used as outgroups.

772

773 **Figure 4.** (A) SDS polyacrylamide gel of soluble crude extract. Lane 1: Molecular mass  
774 markers (in kDa). Lane 2: 200 µg of crude extract. (B) Immunoblotting experiments of crude  
775 extract from cellobiose (Lane 1) fructose (Lane 2), glucose (Lane 3), maltose (Lane 4) and  
776 sucrose (Lane 5) demonstrating the presence of hydrogenases. Molecular mass markers were  
777 given in kDa.







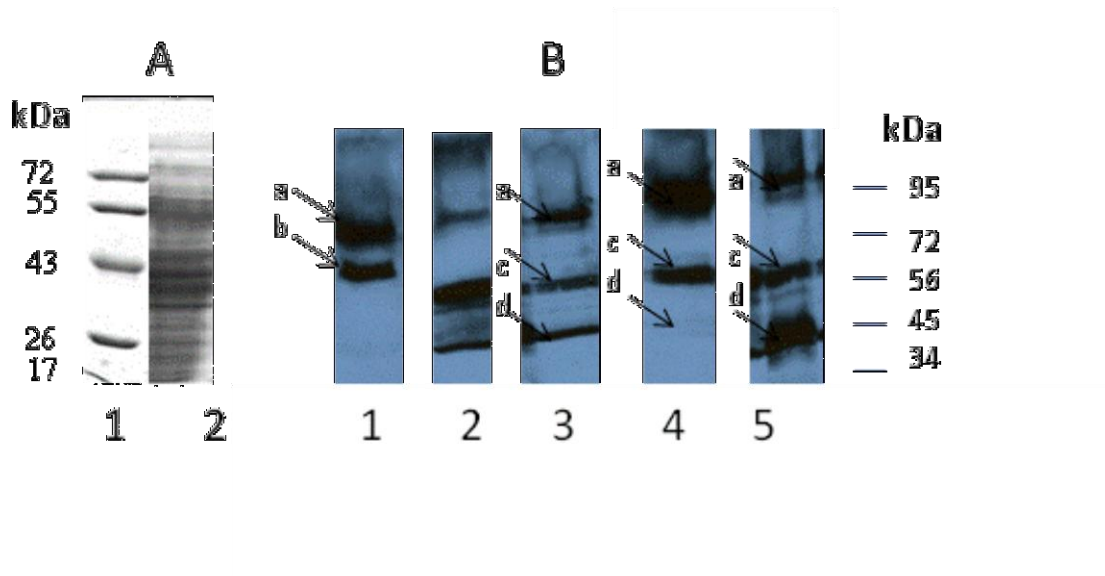




**Table 1. Performance of fermentative H<sub>2</sub> production from different type of carbohydrates**

Substrates	Fructose	Glucose	Sucrose G-( $\alpha$ 1,2)-F	Maltose G-( $\alpha$ 1,4)-G	Cellobiose G-( $\beta$ 1,4)-G	Maltotriose G-( $\alpha$ 1,4)-G-( $\alpha$ 1,4)-G	Statistical significance <sup>b</sup>
<i>P</i> (L-H <sub>2</sub> /L) <sup>a</sup>	2.31 ± 0.21	2.24 ± 0.15	2.16 ± 0.12	2.08 ± 0.08	2.00 ± 0.08	1.85 ± 0.16	*
R <sub>m</sub> (L-H <sub>2</sub> /L/d) <sup>a</sup>	0.91 ± 0.37	0.71 ± 0.19	0.92 ± 0.33	0.45 ± 0.03	0.41 ± 0.04	0.36 ± 0.08	*
$\lambda$ (day) <sup>a</sup>	1.69 ± 0.32	1.66 ± 0.19	1.82 ± 0.29	1.64 ± 0.09	2.04 ± 0.09	2.02 ± 0.10	n.s.
R <sup>2</sup> (%) <sup>a</sup>	99.6 ± 0.4	99.5 ± 0.3	99.3 ± 0.6	98.7 ± 0.1	99.6 ± 0.2	99.3 ± 0.3	n.s.
H <sub>2</sub> yield (mol-H <sub>2</sub> /mol-hexose)	1.84 ± 0.17	1.79 ± 0.12	1.67 ± 0.09	1.65 ± 0.06	1.56 ± 0.06	1.38 ± 0.12	**
R <sub>c</sub> (mL/L)	55.9 ± 20.5	62.8 ± 15.4	30.5 ± 34.3	53.6 ± 35.1	84.4 ± 1.4	41.9 ± 21.5	n.s.
Max. H <sub>2</sub> content (%)	32.5 ± 1.1	34.2 ± 1.0	32.8 ± 0.7	32.7 ± 1.1	32.4 ± 0.6	31.0 ± 1.3	*
Final H <sub>2</sub> content (%)	22.8 ± 0.7	22.7 ± 1.3	27.6 ± 3.5	26.4 ± 2.7	22.9 ± 0.7	25.1 ± 0.8	*
Time when <i>P</i> was reached (days)	7.7 ± 1.2	7.7 ± 1.2	9.7 ± 0.6	9.7 ± 0.6	9.7 ± 0.6	9.7 ± 0.6	*
<b>Final pH</b>	<b>4.0 ± 0.0</b>	<b>4.0 ± 0.0</b>	<b>4.0 ± 0.0</b>	<b>3.9 ± 0.0</b>	<b>4.0 ± 0.0</b>	<b>4.0 ± 0.0</b>	<b>n.s.</b>

<sup>a</sup> Parameters derived from modified Gompertz equation

<sup>b</sup> Significant differences between substrate conditions are indicated by asterisks: \*\*, p<0.005; \*, p<0.05; n.s., not significant (p>0.05).

**Table 2. Metabolite formation in fermentative mixed cultures from different carbohydrates**

Substrates	Acetate		Butyrate		Caproate		Ethanol		Lactate		Bu/Ac ratio	
	(mmoles-Ac/mol-hexose)		(mmoles-Bu/mol-hexose)		(mmoles-Ca/mol-hexose)		(mmoles-Et/mol-hexose)		(mmoles-La/mol-hexose)		<i>P</i> time	Final time
	<i>P</i> time	Final time	<i>P</i> time	Final time	<i>P</i> time	Final time	<i>P</i> time	Final time	<i>P</i> time	Final time	<i>P</i> time	Final time
Fructose	266.7	398.6	473.5	565.4	0.0	0.0	48.5	42.7	7.2	0.0	1.78	1.42
Glucose	245.8	218.0	449.9	310.5	0.0	0.0	45.8	0.0	6.5	0.0	1.83	1.42
Sucrose	370.2	271.3	540.5	333.8	0.0	20.6	59.7	56.2	6.6	0.0	1.46	1.23
Maltose	291.0	266.1	465.7	376.7	8.5	33.0	32.6	28.0	0.0	7.2	1.60	1.41
Cellobiose	309.3	279.7	454.7	327.1	10.8	43.2	78.6	41.4	18.8	0.0	1.47	1.17
Maltotriose	275.9	305.8	426.2	389.8	11.1	10.3	147.0	117.5	28.2	0.0	1.54	1.27

**Table 3. Hydrogenase identification by metaproteomic analysis from Clostridium database.** Proteins were identified by ion trap mass spectrometry from the band cut out from the SDS gel shown in Figure 4.

Band	N°	Protein name <sup>a</sup>	NCBI entry <sup>b</sup>	Coverage <sup>c</sup>	Peptides <sup>d</sup>	Mass <sup>e</sup>
a	1	Chaperonin GroEL	229261799	3.5	3	57.9
	2	Hypothetical protein	229261779	3.5	3	85.9
	3	FlaB	110164831	4.1	2	52.1
	4	<b>Hydrogenase Fe only</b>	220000195	4.5	4	62.5
	5	Chaperonin GroEL	18311271	2.4	2	65
	8	<b>Hydrogenase Fe only</b>	118444478 187779567	2.1	2	54.6
b	1	Conserved protein	28204348	7.6	2	48.5
	2	ATP dependent DNA ligase	219998149	13.4	4	36.8
	3	Putative Na antiporter	126698235	4.5	2	42.2
	4	<b>Ech hydrogenase subunit</b>	220930727	10.5	4	49.5
c	1	Transcript regulator Crp/Fnr	266620955	5.1	3	27.2
	2	SurE	255523330	4	4	27.4
	9	<b>Fe-Hydrogenase</b>	52854761	3.3	3	25.5
	12	<b>Fe-Hydrogenase</b>	255527517	2	1	46.8
d	53	NADH dehydrogenase	149905389	18.3	2	18.6

<sup>a</sup> Protein name is name as given in NCBI database.

<sup>b</sup> NCBI entry is the accession number.

<sup>c</sup> Coverage indicates protein sequence coverage by the matching peptides (in %).

<sup>d</sup> Peptides correspond to the number of different peptides matching to the protein sequence.

<sup>e</sup> Mass indicates the theoretical molecular mass in kDa of the identified protein calculated from the amino acid sequence without possible processing or modifications.